Inorganic Chemistry

pubs.acs.org/IC
Article

Cationic Group 13/14/15 Element Chain Compounds with Pnictogen-Donor Ligands

Published as part of Inorganic Chemistry special issue "Current Advancements in Main Group Chemistry".

Tatiana N. Parfeniuk, Matthias T. Ackermann, Christoph Riesinger, and Manfred Scheer*

Cite This: *Inorg. Chem.* 2026, 65, 10622−10631

ABSTRACT: The reactivity of IDipp·GeH_2BH_2OTf (**1**) (IDipp = 1,3-bis(2,6-diisopropylphenyl)imidazolin-2-ylidene) toward monodentate N-donor and bidentate pnictogen-donor ligands is reported. In the reaction of **1** with triethyl amine, the cationic adduct $[IDipp·GeH_2BH_2·NEt_3]^+$(**2**$^+$) is formed. In contrast, primary and secondary amines exhibit a proton transfer to the germanium center, resulting in the formation of $[IDipp·GeH_3]^+$ (**4**$^+$) and $[IDipp·BH_2·NHR'R'']^+$ (**3**$^+$**a**−**c**) species. DFT calculations reveal that the driving force for the observed difference in reactivity is the tendency of $NHEt_2$ to transfer a proton to **1**, leading to the formation of **3a**, **4**, and $[IDippH]^+$. Pyridine and aminopyridine also form stable adducts $[IDipp·GeH_2BH_2·Py]^+$ (**5**$^+$) and $[IDipp·GeH_2BH_2·DMAP]^+$ (**6**$^+$). Reactions with bidentate ligands (bipyridine and 1,2-bis(diphenylphosphino)ethane) lead to the formation of unprecedented dicationic chains composed of two $[IDipp·GeH_2BH_2]^+$ units connected via the linker to form $[IDipp·GeH_2BH_2·bipy·BH_2GeH_2·IDipp]^{2+}$ (**7**$^{2+}$) and $[IDipp·GeH_2BH_2·dppe·BH_2GeH_2·IDipp]^{2+}$ (**8**$^{2+}$), respectively. All synthesized compounds are characterized by SC-X-ray crystallography, NMR spectroscopy, and mass spectrometry, providing insights into their structural features.

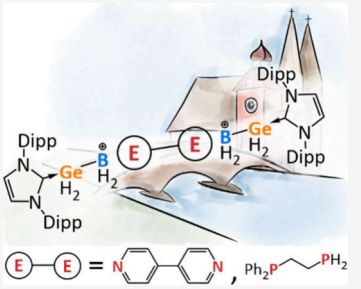

INTRODUCTION

The synthesis of molecular compounds incorporating combinations of group 13, 14, and 15 elements has earned significant attention over the past decades due to their importance in both fundamental chemistry and materials science. Based on the isolobal analogy between the $E^{14}H_2$, $[E^{13}H_2]^-$, and $[E^{15}H_2]^+$ fragments, binary or ternary combinations of these moieties serve as inorganic analogs of hydrocarbons.[1] Thus, such compounds can be regarded as building blocks for inorganic polymers, which are of interest as a rising class of materials with unique features.[2−8] Furthermore, both monomeric and oligomeric compounds are prominent single-source precursors (SSPs) for important materials, such as III−V and IV−V semiconductors.[5,9−16]

Although isoelectronic with hydrocarbons, related main-group element compounds exhibit diverse reactivity due to the higher polarity of E-E' bonds. Since the $[E^{13/14/15}H_2]^{-/0/+}$ moiety possesses both a lone pair of electrons in its valence s-orbital, as well as an empty p-orbital, molecules with different combinations of these fragments tend to oligomerize. To prevent this oligomerization, the respective monomers require additional stabilization − either sterically or electronically. Steric protection is achieved by employing bulky organic substituents, e.g. polyalkylphenyl groups, which shield the reactive sites and prevent oligomerization and enhance the stability but disfavors a subsequent reactivity.[17−23]

A powerful strategy to suppress undesired reactivity is a donor−acceptor stabilization, for instance with electron-rich N-heterocyclic carbenes (NHCs). The donor−acceptor approach has enabled the stabilization of the low valent tetrylenes, where the ER_2 (E = Si, Ge, Sn) fragment simultaneously possesses a lone pair of electrons and an empty p-orbital, thereby exhibiting ambiphilic behavior.[24−28] NHC-stabilized tetrylenes have become promising building blocks for introducing Si or Ge into mixed-element molecules, and their further functionalization has been excessively studied.[29−34] Notably, Rivard and co-workers demonstrated this donor−acceptor strategy by isolating a Ge(II) dihydride complex stabilized by a NHC and a borane as Lewis acid, followed by the first stable Si(II) dihydride analogue (Scheme 1a).[28,35,36] Moreover, donor−acceptor stabilization has proven essential for isolating binary main-group compounds such as $R_2E^{13}−E^{15}R'_2$ and for achieving control over their polymerizations and oligomerizations.[37−41] Significant contributions for the stabilization of parent $H_2E^{13}−E^{15}H_2$ compounds were made by our group, including the synthesis of combinations involving heavier group 13 and 15 elements (Scheme 1a).[42−50] In contrast to binary main-group element combinations,

Received: February 3, 2026
Revised: March 17, 2026
Accepted: April 7, 2026
Published: May 4, 2026

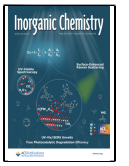

https://doi.org/10.1021/acs.inorgchem.6c00556
Inorg. Chem. 2026, 65, 10622−10631

Scheme 1[a]

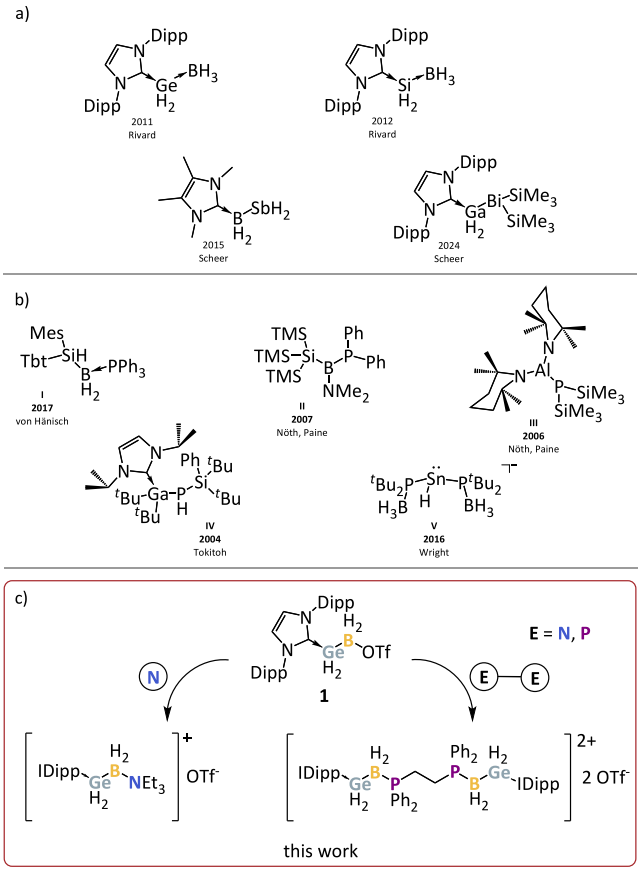

[a]((a) Examples of donor−acceptor stabilized low valent groups 13/14 and 13/15 element compounds; (b) selected examples of linear mixed group 13/14/15 elements compounds; (c) functionalization pathways of IDipp·GeH$_2$BH$_2$OTf (formal charges are omitted but the positive charge is located on the germanium atom). Mes = 2,4,6-trimethylphenyl, Tbt = 2,4,6-tris[bis(trimethylsilyl)methyl]phenyl, TMS = trimethylsilyl, Dipp = 2,6-diisopropylphenyl.

ternary compounds containing elements from three different groups are much rarer and mainly represented by cyclic compounds or species containing cyclic fragments. Early examples include cluster or cage compounds with combinations such as B−Ge−P or B−Sn−P.[51−53] More recently, cyclic frameworks featuring three different main-group elements have been isolated.[54−64] Considering linear heteroatomic chains derived via insertion or addition reactions, the number of known examples is even smaller (Scheme 1b).[17,65−79] For instance, some of the earlier examples from the groups of Tokitoh, Pain and Nöth involved lighter group 13 and 14 elements such as boron and silicon (**I**−**II**). Later, chain compounds with heavier congeners, including gallium and tin, were achieved by the groups of von Hänisch (**IV**) and Wright (**V**).[74,75] This scarcity highlights the challenge and significance of assembling three different main-group element types in a controlled linear arrangement and show the need of organic substituents for its stabilization. Recently in a collaboration between the Rivard and our group, the synthesis of the cationic precursor [IDipp·GeH$_2$BH$_2$]$^+$ was achieved. This compound has proven its utility as a building block for group 13/14/15 mixed-element chains with P and As donors, respectively.[80−82] Therefore, the question arises as to whether this reactivity could be expanded to N-donors and even bidentate ligands, potentially leading to the formation of unique cationic chain compounds (Scheme 1c). Herein, we report on the expansion of the reactivity of [IDipp·GeH$_2$BH$_2$]$^+$ toward monodentate N-donor and bidentate pnictogen-donor ligands to obtain novel group 13/14/15 compounds possessing parent group 13/14 parts.

RESULTS AND DISCUSSION

Reactivity of 1 toward Amines

The reactivity of IDipp·GeH$_2$BH$_2$OTf (**1**) toward amines was investigated, starting with the tertiary amine NEt$_3$ (Scheme 2).

Scheme 2. Synthesis of 2, 3a−b, 5, 6 by the Reaction of IDipp·GeH$_2$BH$_2$OTf (1)[A]

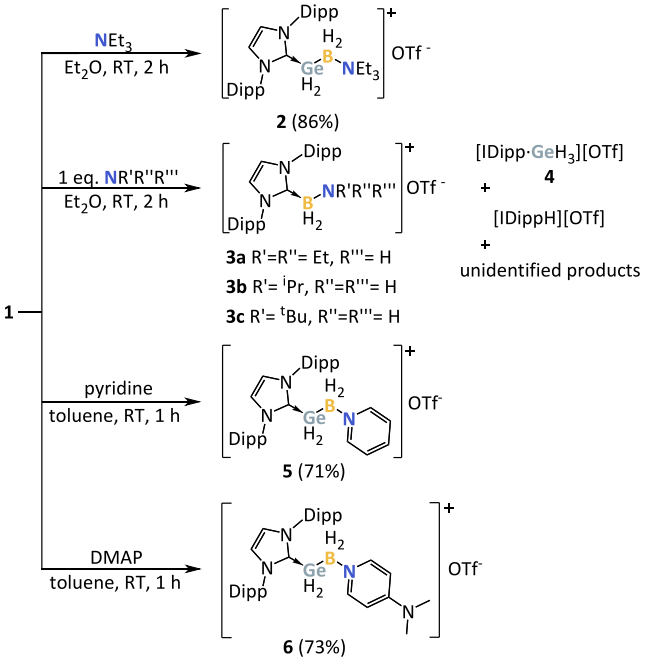

[A]Isolated yields are given in parentheses. Formal charges are omitted but the positive charge is located on the germanium atom.

The reaction proceeds in Et$_2$O at room temperature to give [IDipp·GeH$_2$BH$_2$·NEt$_3$][OTf] (**2**) in excellent yield (86%). In the crystal structure of **2** (Figure 1), the B1−N1 bond length of 1.609(2) Å is slightly longer than the B−N bond in ammonia borane H$_3$N→BH$_3$ (1.56(5) Å).[83] The Ge−B bond amounts to 2.0734(18) Å and is slightly longer than that in the neutral compound IDipp·GeH$_2$BH$_3$ [2.053(3) Å], but nearly identical to the corresponding bond in **1** [2.081(3) Å].[28,80] Notably, no short contacts between the cation and the triflate anion are observed. In contrast to the adduct formation with tertiary NEt$_3$, the reaction of **1** with secondary (NHEt$_2$) and primary (NH$_2$^{i}Pr, NH$_2$^{t}Bu) amines affords complicated product mixtures, containing [IDipp·BH$_2$·NHEt$_2$][OTf] (**3a**), [IDipp·BH$_2$·NH$_2$^{i}Pr][OTf] (**3b**) and [IDipp·BH$_2$·NH$_2$^{t}Bu]-[OTf] (**3c**) respectively, as well as [IDipp·GeH$_3$][OTf] (**4**) and [IDippH][OTf] (Scheme 2). This type of reactivity was observed for different stoichiometric ratios of **1** to amine (1:1 and 1:2), with **3a**−**3c** being the main products in each case. However, due to severe overlap of the ^{1}H NMR signals of **3**, **4** and [IDippH][OTf], as well as the presence of other unidentified side products, it was not possible to doubtlessly determine the ratio of products. Single crystals of compounds

https://doi.org/10.1021/acs.inorgchem.6c00556
Inorg. Chem. 2026, 65, 10622−10631

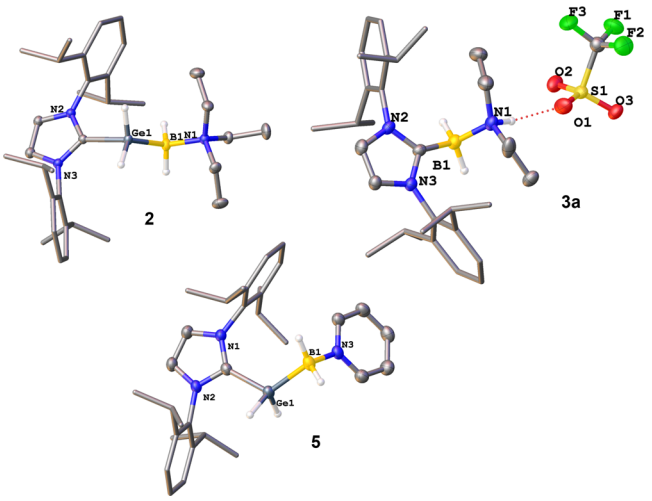

Figure 1. Molecular structures of the cations of **2** (top left) and **5** (bottom), respectively, and molecular structure of **3a** (top right) in the solid state with anisotropic displacement ellipsoids at the 50% probability level. Counterions and hydrogen atoms bound to carbon are omitted for clarity.

3a–**3c** suitable for XRD analysis were picked from the mixture of crystals with **4** and [IDippH][OTf]. In the crystal structures of **3a**–**3c**, hydrogen bonding between the amine proton and the oxygen atom of the triflate anion was observed. The C–B bonds in **3a** (1.629(5) Å), **3b** (1.603(2) Å) and **3c** (1.612(2) Å) are significantly elongated, compared to a neutral adduct IDipp·BH_3 (1.585(4) Å) due to the σ-donation from amines, that reduces the Lewis acidity of boron center and weakens the NHC→B donation.[84] **3a** possesses the longest bond, reflecting the stronger σ-donation from the $NHEt_2$, **3b** and **3c** have shorter bonds due to weaker σ-donation of $NH_2{}^i$Pr and $NH_2{}^t$Bu, however the C–B bond in **3c** is slightly longer, due to steric repulsion. The B1–N1 bond lengths amount to 1.604(5) Å, 1.604(2) Å, and 1.6074(18) Å for **3a**, **3b** and **3c**, respectively. They are shorter than the B–N bond in **2**. Based on the identified products of this reaction, it can be proposed that the interaction of **1** with secondary and primary amines leads to protonation of the "GeH_2" moiety and elimination of [IDipp·GeH_3][OTf]. Due to the interaction of the triflate anion with amine protons, it was assumed that the triflate anion may play a decisive role in the protonation process of the germanium center. To test this, the counterion in **1** was exchanged with $[BAr^F]^-$ or $[TEF]^-$ (BAr^F = $[B(C_6F_5)_4]^-$, TEF = $[Al(OC(CF_3)_3)_4]^-$) by addition of $KBAr^F$ or LiTEF in diethyl ether, monitored by NMR spectroscopy and mass spectrometry (cf. Supporting Information). Subsequently, one equivalent of NH^iPr_2 was added to this mixture. However, according to the ESI mass spectrum of the reaction mixture, no amine complex but the formation of the etherate $[IDipp{\cdot}GeH_2BH_2{\cdot}OEt_2]^+$ was observed. This suggests that the interaction between the triflate anion and the cationic counterpart may play a crucial role in the stabilization of the main-group element chain. When the counterion is exchanged by weakly coordinating anions $[BAr^F]^-$ or $[TEF]^-$, an Et_2O molecule coordinates to the boron atom, forming a very stable adduct $[IDipp{\cdot}GeH_2BH_2{\cdot}OEt_2]^+$, which was detected by mass spectrometry. Attempts to carry out the anion exchange in 1,2-difluorobenzene, in order to avoid solvent coordination, resulted only in decomposition: in the ^{1}H NMR spectra of the reaction mixtures with both $[BAr^F]^-$ and $[TEF]^-$, mostly the signals of **4** were observed, and in the ^{11}B NMR spectra no signals attributable to a BH_2 moiety could be detected (cf. Supporting Information).

To understand the difference in reactivity of **1** with tertiary (NEt_3) and secondary ($NHEt_2$) amines, DFT calculations were performed at the B3LYP/def2-TZVP level of theory (Table 1). As products of the reaction of **1** with $NHEt_2$ the cationic compounds $[IDipp{\cdot}BH_2{\cdot}NHEt_2]^+$ (**3a**), $[IDipp{\cdot}GeH_3]^+$ (**4**) and $[IDippH]^+$ were detected by NMR spectroscopy and mass spectrometry. However, not all of the products could be identified, and therefore the complete reaction pathway could not be proposed. Thus, several potential processes leading to the formation of the cations $[IDipp{\cdot}BH_2{\cdot}NHEt_2]^+$ (**3a**), $[IDipp{\cdot}GeH_3]^+$ (**4**) and $[IDippH]^+$ were investigated. (Table 1). The latter imidazolium salt might arise from protonation of **1** by $NHEt_2$, while a formal "GeH_2" moiety may be generated during the process, giving $[IDipp{\cdot}GeH_3]^+$ (**4**). According to the computations, the formation of the expected products $[IDipp{\cdot}GeH_2BH_2{\cdot}(amine)]^+$ with both NEt_3 and $NHEt_2$ is energetically favorable (Table 1, reactions 1 and 4, respectively). However, in the case of NEt_3 the formation of a $[IDipp{\cdot}BH_2{\cdot}(amine)]^+$ species and the "GeH_2" moiety is endergonic (Table 1, reaction 2), whereas for $NHEt_2$ the same process is exergonic (Table 1, reaction 5). Formation of $[IDipp{\cdot}GeH_3]^+$ (**4**) in the reaction of **1** with $[IDippH]^+$ and NEt_3 or $NHEt_2$ (Table 1, reactions 3 and 6, respectively) is also thermodynamically favorable. In case of the secondary amine $NHEt_2$, there is another type of reactivity possible: protonation of **1** by $NHEt_2$, with formation of $[IDipp{\cdot}GeH_3]^+$ (**4**) and the aminoborane BH_2NEt_2 (Table 1, reaction 7). This process is also highly energetically favorable. Thereby, out of

Table 1. Thermodynamic characteristics for Different Gas Phase Processes[a]

Process	ΔH°_{298}	ΔS°_{298}	ΔG°_{298}
1 + NEt_3 = **2** (1)	−158	−221	−92
1 + NEt_3 = $[IDipp{\cdot}BH_2{\cdot}NEt_3]^+$ + GeH_2 (2)	−2	−91	25
1 + NEt_3 + $[IDippH]^+$ = $[IDipp{\cdot}BH_2{\cdot}NEt_3]^+$ + **4** (3)	−128	−280	−45
1 + $NHEt_2$ = $[IDipp{\cdot}GeH_2BH_2{\cdot}NHEt_2]^+$ (4)	−165	−201	−106
1 + $NHEt_2$ = **3a** + GeH_2 (5)	−36	−58	−19
1 + $NHEt_2$ + $[IDippH]^+$ = **3a** + **4** (6)	−162	−246	−89
1 + $NHEt_2$ = 4 + BH_2NEt_2 (7)	−154	−20	−148

[a]Standard reaction enthalpies ΔH°_{298} and Gibbs energies ΔG°_{298} in kJ mol^{-1}, standard reactions entropies ΔS°_{298} in J mol^{-1} K^{-1}. B3LYP/def2-TZVP level of theory.

https://doi.org/10.1021/acs.inorgchem.6c00556
Inorg. Chem. 2026, 65, 10622–10631

three possible reactivity pathways proposed for the NEt_3 reaction (Table 1, reactions 1−3), the most exergonic is the reaction 1, leading to the formation of [IDipp·GeH_2BH_2·NEt_3][OTf] (**2**). On the contrary, for $NHEt_2$ the most exergonic process out of reactions 4−7 (Table 1), is the formation of $[IDipp{\cdot}GeH_3]^+$ (**4**) and the aminoborane BH_2NEt_2 (Table 1, reaction 7). Notably, the aminoborane can further oligomerize, acting as an additional driving force for this side reaction. This distinct reactivity pattern agrees with the experimental observations.

Reactivity of 1 toward Pyridine-Based Compounds

Since the amine proton appeared to be responsible for the elimination of [IDipp·GeH_3][OTf], the reactivity of IDipp·GeH_2BH_2OTf (**1**) toward pyridine-based compounds was investigated (Scheme 2). The successful formation of the pyridine (Py) adduct [IDipp·GeH_2BH_2·Py][OTf] (**5**) was confirmed both by NMR spectroscopy and SC-XRD (Figure 2). Single crystals suitable for X-ray analysis were obtained by layering a concentrated DCM solution of the product with a 3-fold excess of *n*-hexane and storage at +9 °C. For **5**, the characteristic ^{1}H NMR signals of Py were observed in the aromatic region at δ = 7.43, 7.83, and 7.94 ppm. The formation of the DMAP adduct [IDipp·GeH_2BH_2·DMAP][OTf] (**6**) was likewise confirmed by NMR spectroscopy, which showed characteristic signals for the methyl groups and the pyridine ring of DMAP in the ^{1}H NMR spectrum at δ = 3.04, 6.38, and 7.35 ppm, respectively. In the crystal structure of **5**, the B1−N1 distance amounts to 1.574(2) Å, which is significantly shorter than that in the triethylamine complex **2**.

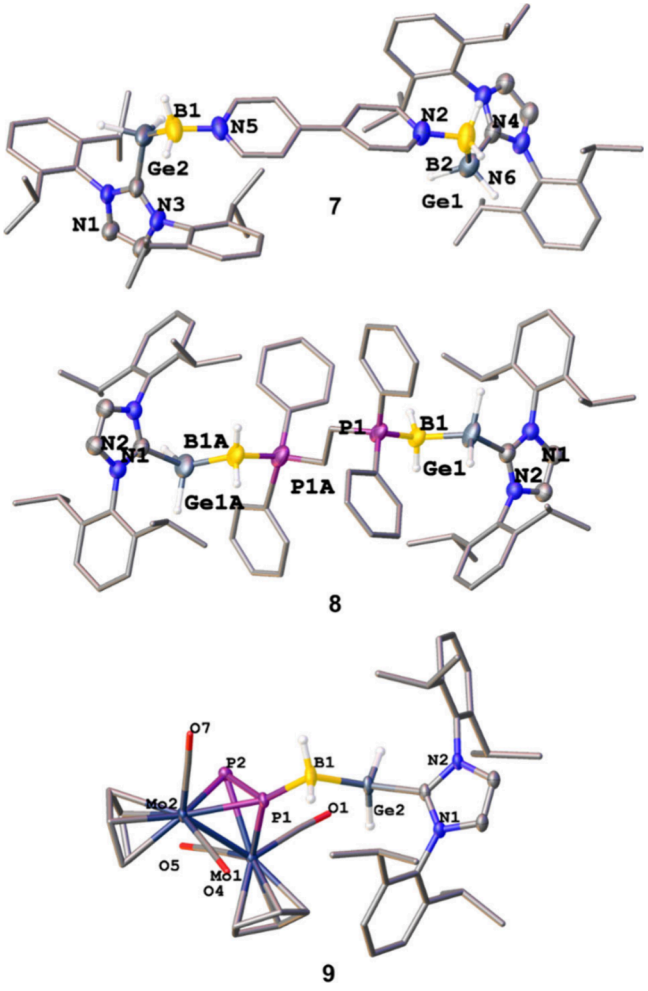

Figure 2. Molecular structures of the dications of **7**, **8**, and **9** in the solid state with anisotropic displacement ellipsoids at a 50% probability level. Counterions and hydrogen atoms bound to carbon are omitted for clarity.

Reactivity of 1 toward Bidentate Linkers

Furthermore, the possibility of forming dicationic chains by the reaction of the precursor IDipp·GeH_2BH_2OTf (**1**) with bidentate linkers was examined. First, the reactivity toward TMEDA (tetramethylethylenediamine) was studied. However, as evident from the ^{11}B NMR spectrum (cf. Supporting Information), TMEDA abstracts the "$[BH_2]^+$" moiety from the chain by chelation, giving the product $[TMEDA{\cdot}BH_2]^+$, which exhibits a characteristic signal at δ = 6.2 ppm.[85] The cation $[IDipp{\cdot}GeH_3]^+$ is formed as a byproduct of this reaction. Since TMEDA, as a flexible linker, is able to cleave the Ge−B bond, rigid linkers were then employed in order to access dicationic chain compounds. The reaction of two equivalents of IDipp·GeH_2BH_2OTf with 4,4'-bipyridine (bipy) in toluene at room temperature led to the 2:1 complex [IDipp·GeH_2BH_2·bipy·BH_2GeH_2·IDipp][OTf]$_2$ (**7**) (Scheme 3), which was characterized by NMR spectroscopy, SC-XRD and mass spectrometry. In the ^{1}H NMR spectrum of **7**, the characteristic doublet signals of bipy appear at δ = 7.96 ppm and δ = 8.00 ppm, respectively. The integrals of the proton signals also confirm the 2:1 ratio of IDipp to bipy. The B1−N5 and B2−N2 bond lengths in **7** (Figure 2) are the same at 1.585(4) Å, despite the absence of crystallographic symmetry, a value nearly identical to the corresponding bond length in the Py adduct **5**. Reaction of IDipp·GeH_2BH_2OTf with 1,2-bis(diphenylphosphino)-ethane (dppe) in toluene at room temperature afforded the 2:1 complex [IDipp·GeH_2BH_2·dppe·BH_2GeH_2·IDipp][OTf]$_2$ (**8**) (Scheme 3). In the crystal structure of **8** (Figure 2) the two P−B bonds with distances of 1.891(18) Å and 1.948(19) Å, respectively, differ slightly. However, considering the relatively large standard deviations arising from the pro-

Scheme 3. Synthesis of 7, 8, and 9 by the Reaction of IDipp·GeH_2BH_2OTf (1) with Different Bidentate Linkers[a]

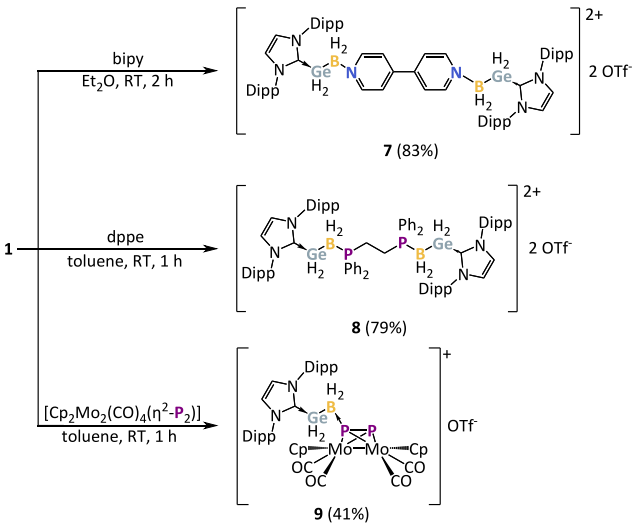

[a]Isolated yields are given in parentheses. Formal charges are omitted but the positive charge is located on the germanium atom.

https://doi.org/10.1021/acs.inorgchem.6c00556
Inorg. Chem. 2026, 65, 10622−10631

nounced disorder in the central chain fragment, this difference should be interpreted with caution. Moreover, the ^{31}P NMR spectrum at room temperature exhibits only one broad signal at δ = 19.2 ppm ($\omega_{1/2}$ = 90 Hz), which could not be resolved even at −80 °C ($\omega_{1/2}$ = 74 Hz), indicating that both phosphorus atoms are chemically equivalent. Interestingly, the ^{1}H NMR spectrum of **7** containing the bipy linker shows a set of two doublets for the methine protons of the isopropyl groups of the IDipp carbene, whereas the dppe complex **8** gives only one doublet. This difference can be attributed to the free rotation along the dppe backbone.

Other potential phosphorus-centered bidentate linkers were also tested in reactions with IDipp·GeH_2BH_2OTf (**1**). The tetrahedral complex $[Cp_2Mo_2(CO)_4(\eta^2\text{-}P_2)]$[86] was reacted with IDipp•GeH_2BH_2OTf in both 1:2 and 1:1 stoichiometries. However, in both cases only the one-fold addition product $[Cp_2Mo_2(CO)_4(\eta^2\text{-}P_2)\cdot BH_2GeH_2\cdot IDipp][OTf]$ (**9**) was obtained (Scheme 3). The ^{31}P NMR spectrum of **9** shows two doublets at δ = −18.5 ppm and −158.3 ppm corresponding to two inequivalent P atoms, coupled to each other with $^{1}J_{P,P}$ = 505 Hz. The single crystal X-ray structure analysis of **9** also confirms the formation of the 1:1 complex. Two molecules of **9** crystallize in the asymmetric unit, exhibiting the B−P bond lengths of 1.953(3) Å and 1.949(3) Å, respectively, which are equal within an experimental error. Those values are similar to the B−P bond lengths in **8**. However the P-P bonds of the distances 2.0725(8) Å and 2.0742(8) Å in **9** are slightly shorter than in the parent compound $[Cp_2Mo_2(CO)_4(\eta^2\text{-}P_2)]$ 2.079(2) Å, indicating a polarization of the P−P bond.[86] The moderate nucleophilicity of $[Cp_2Mo_2(CO)_4(\eta^2\text{-}P_2)]$ may explain why the reaction with a second equivalent does not proceed. The reaction of **1** with white phosphorus was studied subsequently. However, no reaction was observed, even after prolonged reflux in THF, consistent with the fact that white phosphorus is a very weak nucleophile. The tetrahedral arsenic complex $[Cp^*_2Mo_2(CO)_4(\eta^2\text{-}As_2)]$[87] was also treated with two equivalents of **1**, but only the formation of [IDipp·GeH_3][OTf] as a decomposition product was observed. The nucleophilicity of such tetrahedral pnictogen complexes decreases down the group, and the energy of the lone pairs at the arsenic atoms was shown to be relatively low.[88,89] Therefore, the diarsenic compound is not reactive enough to bind **1**.

CONCLUSION

The broad synthetic versatility of the cationic precursor $[IDipp\cdot GeH_2BH_2]^+$ has been clearly demonstrated through its ability to access a wide range of novel structurally diverse group 13/14/15 element chain compounds. Its rich and tunable reactivity toward various pnictogen-donor ligands enabled the isolation of several new, well-defined mono- and dicationic complexes, highlighting its utility as a modular building block for unprecedented mixed main-group systems. Reactions with tertiary amines, pyridine, and aminopyridine proceeded cleanly to afford the stable monocationic adducts $[IDipp\cdot GeH_2BH_2\cdot NEt_3][OTf]$ (**2**), [IDipp·GeH_2BH_2·Py][OTf] (**5**) and [IDipp·GeH_2BH_2·DMAP][OTf] (**6**) in which the donor ligand coordinates to the boron center. In contrast, secondary and primary amines exhibit fundamentally different reactivity toward $[IDipp\cdot GeH_2BH_2]^+$, readily inducing proton transfer to the germanium center. This process results in the formation of $[IDipp\cdot GeH_3]^+$ (**4**) and aminoborane-derived cations $[IDipp\cdot BH_2\cdot NHR'R'']^+$ (**3a**−**3b**), underscoring the critical influence of the amine proton on the reaction outcome. Density functional theory (DFT) calculations were performed to rationalize these experimentally observed trends and provided valuable insight into the energetic preference for adduct formation versus proton transfer pathways. Furthermore, the use of bidentate linkers, such as rigid 4,4'-bipyridine (bipy) and flexible 1,2-bis(diphenylphosphino)ethane (dppe), enabled the assembly of unprecedented dicationic chain compounds $[IDipp\cdot GeH_2BH_2\cdot bipy\cdot BH_2GeH_2\cdot IDipp][OTf]_2$ (**7**) and $[IDipp\cdot GeH_2BH_2\cdot dppe\cdot BH_2GeH_2\cdot IDipp][OTf]_2$ (**8**). These species feature two $[IDipp\cdot GeH_2BH_2]^+$ units bridged by a bidentate ligand, representing a novel structural motif within mixed group 13/14/15 element chemistry. In addition, the reactivity of **1** toward the tetrahedral pnictogen complex $[Cp_2Mo_2(CO)_4(\eta^2\text{-}P_2)]$ was explored, resulting exclusively in the formation of the 1:1 adduct $[Cp_2Mo_2(CO)_4(\eta^2\text{-}P_2)\cdot BH_2GeH_2\cdot IDipp][OTf]$ (**9**). All isolated compounds were comprehensively characterized by multinuclear NMR spectroscopy, single-crystal X-ray diffraction, and mass spectrometry, providing detailed insight into the bonding environments and structural motifs of these novel main-group element chain compounds.

EXPERIMENTAL SECTION

Working Techniques and Materials

All the manipulations were carried in the inert atmosphere of dry argon using the glovebox or Schlenk techniques. The argon gas was purified from traces of H_2O and O_2 by passing it through the BASF R 3−11 ($CuO/MgSiO_3$) catalyst, concentrated H_2SO_4, and then Orange Gel and Sicapent supported on pumice stone. Et_2O, CH_2Cl_2, toluene, hexane and pentane were purified using an MBraun SPS-800 solvent purification system, degassed at room temperature, and stored over molecular sieves for at least 48 h. Deuterated solvents and o-DFB were dried over CaH_2, distilled under argon and stored over the molecular sieves. The NMR spectra were recorded on a Bruker Avance 400 spectrometer (^{1}H: 400.13 MHz, ^{31}P: 161.976 MHz, ^{11}B: 128.378 MHz, ^{19}F: 376.498 MHz) or Avance 500 (^{1}H: 500.178 MHz; ^{31}P: 202.476 MHz, ^{11}B: 160.477 MHz, ^{19}F: 470.637 MHz) with δ [ppm] referenced to external $SiMe_4$ (^{1}H), H_3PO_4 (^{31}P), $F_3B\cdot Et_2O$ (^{11}B). Mass spectra were recorded on an Agilent Q-TOF 6540 UHD (ESI-MS) and a Jeol AccuTOF GCX spectrometer (LIFDI-MS). Elemental analyses were determined with a Vario Micro Cube apparatus. The compounds IDipp·GeH_2BH_2OTf[80] and $Cp_2Mo_2(CO)_4(\eta^2\text{-}P_2)$[86] were prepared according to literature procedures. NEt_3, $NHEt_2$, $NH_2{}^{i}Pr$, $NH_2{}^{t}Bu$, pyridine (Py), 4-(dimethylamino)pyridine (DMAP), 4,4′-bipyridine (bipy) and 1,2-bis(diphenylphosphino)ethane (dppe) were obtained from Sigma-Aldrich. $NHEt_2$, $NH_2{}^{i}Pr$, $NH_2{}^{t}Bu$ and pyridine were used to prepare stock solutions in toluene, which were stored over the molecular sieves.

Safety Statement

No uncommon hazards are noted.

Synthetic Procedures

[IDipp•GeH_2BH_2•NEt_3][OTf] (2). IDipp·GeH_2BH_2OTf (1) (125 mg, 0.2 mmol, 1 equiv) was dissolved in 10 mL of Et_2O, then NEt_3 (25 mg, 0.25 mmol, 1.25 equiv) was added to the solution dropwise. The reaction mixture was stirred for two hours, then the mother liquor was decanted and the residue washed with 5 mL of Et_2O. All volatiles were removed *in vacuo* and the product [IDipp·GeH_2BH_2•NEt_3][OTf] (2) could be isolated as a white powder (125 mg, 86%). To obtain crystals suitable for X-ray analysis a concentrated DCM solution of the product was layered with 3-fold excess of *n*-hexane and stored at +9 °C. **^{1}H NMR** (CD_2Cl_2, 500 MHz, 298 K): δ [ppm] = 0.95 (t, 9H, $^{3}J_{H,H}$ = 7.3 Hz, CH_2CH_3), 1.23 (d, 12H, $^{3}J_{H,H}$ = 6.8 Hz, $CH(CH_3)_2$), 1.37 (d,12H, $^{3}J_{H,H}$ = 6.7 Hz,

https://doi.org/10.1021/acs.inorgchem.6c00556
Inorg. Chem. 2026, 65, 10622−10631

$CH(CH_3)_2$), 1.54 (br, 2H, BH_2), 2.40 (h, 4H, $^3J_{H,H}$ = 6.8 Hz, $CH(CH_3)_2$), 2.56 (t, 6H, $^3J_{H,H}$ = 7.3 Hz, CH_2CH_3), 3.57 (m, 2H, GeH_2), 7.43 (d, 4H, $^3J_{H,H}$ = 7.9 Hz, Ar*H*), 7.61 (s, 2H, N−C*H*), 7.64 (t, 2H, $^3J_{H,H}$ = 7.9 Hz, Ar*H*). **^{11}B NMR** (CD_2Cl_2, 160.5 MHz, 298 K): δ [ppm] = −15.7 (t, br, BH_2). **^{11}B{^{1}H} NMR** (CD_2Cl_2, 160.5 MHz, 298 K): δ [ppm] = −15.7 (s, br, BH_2). **^{19}F NMR** (CD_2Cl_2, 470 MHz, 298 K): δ [ppm] = −79.09 (s, CF_3). **ESI-MS** (pos. mod., o-DFB): *m*/*z* = 578.37 (100%, [IDipp·GeH_2BH_2·NEt_3]$^+$); **ESI-MS** (neg. mod., o-DFB): *m*/*z* = 148.95 (100%, [CF_3SO_3]$^-$). **Elemental analysis** (%) calculated for $C_{37}H_{55}N_3GeBF_3O_3S$: C: 56.22, H: 7.63, N: 5.79, S: 4.41; found: C: 56.23, H: 7.58, N: 5.63, S: 4.18.

[IDipp•BH_2•$NHEt_2$][OTf] (3a). IDipp·GeH_2BH_2OTf (**1**) (63 mg, 0.1 mmol, 1 equiv) was dissolved in 10 mL of toluene, then the stock solution of $NHEt_2$ (0.1 mmol, 1 equiv) was added to the reaction mixture dropwise. The reaction mixture was stirred for two hours, then all the volatiles were removed, and the residue was washed with 5 mL of *n*-hexane. The solids were dried in vacuo and the mixture of products [IDipp·BH_2•$NHEt_2$][OTf] (**3a**), [IDipp•GeH_3][OTf] (**4**) and [IDippH][OTf] could be isolated as a white powder. To obtain crystals of **3a** suitable for the X-ray analysis the concentrated DCM solution of the product was layered with 3-fold excess of hexane and stored at +9 °C. Due to the severe imposition of the ^{1}H signals from IDipp-carbene of **3a**, **4** and [IDippH][OTf] a full assignment of the signals becomes complicated. However, the presence of those compounds can be determined by the $NHEt_2$ signals of **3a**, GeH_3 hydrides signal from **4** (δ = 4.00 ppm)[80] and the imidazolium proton signal of [IDipp*H*][OTf] (δ = 9.10 ppm). **^{1}H NMR** (CH_2Cl_2/C_6D_6, 500 MHz, 298 K): δ [ppm] = 0.77 (t, 6H, $^3J_{H,H}$ = 7.1 Hz, $NH(CH_2CH_3)_2$), 1.17 (d, 12H, $^3J_{H,H}$ = 6.8 Hz, $CH(CH_3)_2$), 1.30 (d,12H, $^3J_{H,H}$ = 6.9 Hz, $CH(CH_3)_2$), 1.82 (br, 2H, BH_2), 2.35 (m, $CH(CH_3)_2$), 2.47 (m, $NH(CH_2CH_3)_2$), 3.24 (s, $NH(CH_2CH_3)_2$), 7.37 (d, 4H, $^3J_{H,H}$ = 7.8 Hz, Ar*H*), 7.60 (s, N−C*H*), 7.61 (t, Ar*H*). **^{11}B NMR** (CH_2Cl_2/C_6D_6, 160.5 MHz, 298 K): δ [ppm] = −16.2 (t, br, BH_2). **^{11}B{^{1}H} NMR** (CH_2Cl_2/C_6D_6, 160.5 MHz, 298 K): δ [ppm] = −16.2 (s, br, BH_2). **^{19}F NMR** (CH_2Cl_2/C_6D_6, 470 MHz, 298 K): δ [ppm] = −79.09 (s, CF_3). **ESI-MS** (pos. mod., o-DFB): *m*/*z* = 474.31 (100%, [IDipp·GeH_2BH_2·$NHEt_2$]$^+$).

[IDipp•BH_2•$NH_2{}^i$Pr][OTf] (3b). IDipp·GeH_2BH_2OTf (**1**) (63 mg, 0.1 mmol, 1 equiv) was dissolved in 10 mL of toluene, then a stock solution of $NH_2{}^i$Pr (0.1 mmol, 1 equiv) was added dropwise to the reaction mixture. The reaction mixture was stirred for two hours, then all the volatiles were removed and the residue was washed with 5 mL of hexane. Then the volatiles were removed in vacuo and the mixture of products [IDipp·BH_2•$NH_2{}^i$Pr][OTf] (**3b**), [IDipp•GeH_3][OTf] (**4**) and [IDippH][OTf] could be isolated as a white powder. To obtain crystals of **3b** suitable for the X-ray analysis, a concentrated DCM solution of the product was layered with 3-fold excess of *n*-hexane and stored at +9 °C. Due to the severe imposition of the ^{1}H signals from IDipp carbene of **3b**, **4**, [IDippH][OTf] and ^{i}Pr group of $NH_2{}^i$Pr a full assignment of the signals becomes complicated. However, the presence of those compounds can be determined by the $NH_2{}^i$Pr signal of **3b**, GeH_3 hydrides signal from **4** (δ = 3.93 ppm)[80] and the imidazolium proton signal of [IDipp*H*][OTf] (δ = 8.95 ppm). **^{1}H NMR** (CD_2Cl_2, 400 MHz, 298 K): δ [ppm] = 1.04 (d, 6H, $^3J_{H,H}$ = 6.8 Hz, $NH_2CH(CH_3)_2$), 1.08 (d, 12H, $^3J_{H,H}$ = 6.8 Hz, $CH(CH_3)_2$), 1.22 (d,12H, $^3J_{H,H}$ = 6.9 Hz, $CH(CH_3)_2$), 2.24 (s, 2H, $NH_2CH(CH_3)_2$), 2.18(m, $NH_2CH(CH_3)_2$), 2.31 (h, 4H, $^3J_{H,H}$ = 6.7 Hz, $CH(CH_3)_2$), 2.63 (br, 2H, BH_2), 7.28 (d, 4H, $^3J_{H,H}$ = 8.0 Hz, Ar*H*), 7.36 (s, N−C*H*), 7.48 (t, 2H, $^3J_{H,H}$ = 7.7 Hz, Ar*H*). **^{11}B NMR** (CD_2Cl_2, 128 MHz, 298 K): δ [ppm] = −8.2 (t, br, $^1J_{B,H}$= 100 Hz, BH_2). **^{11}B{^{1}H} NMR** (CD_2Cl_2, 128 MHz, 298 K): δ [ppm] = −8.2 (s, br, BH_2). **^{19}F NMR** (CD_2Cl_2, 376.5 MHz, 298 K): δ [ppm] = −76.24 (s, CF_3). **ESI-MS** (pos. mod., o-DFB): *m*/*z* = 460.39 (100%, [IDipp·GeH_2BH_2·$NH_2{}^i$Pr]$^+$).

[IDipp•BH_2•$NH_2{}^t$Bu][OTf] (3c). IDipp·GeH_2BH_2OTf (**1**) (63 mg, 0.1 mmol, 1 equiv) was dissolved in 10 mL of toluene, then a stock solution of $NH_2{}^t$Bu (0.1 mmol, 1 equiv) was added dropwise to the reaction mixture. The reaction mixture was stirred for two hours, then all the volatiles were removed and the residue was washed with 5 mL of *n*-hexane. The volatiles were removed in vacuo and the mixture of products [IDipp·BH_2·$NH_2{}^t$Bu][OTf] (**3c**), [IDipp·GeH_3][OTf] (**4**) and [IDippH][OTf] could be isolated as a white powder. To obtain crystals of **3c** suitable for the X-ray analysis, a concentrated DCM solution of the product was layered with 3-fold excess of *n*-hexane and stored at +9 °C. Due to the severe imposition of the ^{1}H signals from IDipp carbene of **3b**, **4**, [IDippH][OTf] and ^{i}Pr group of $NH_2{}^i$Pr a full assignment of the signals becomes complicated. However, the presence of those compounds can be determined by the $NH_2{}^i$Pr signal of **3b**, GeH_3 hydrides signal from **4** (δ = 4.58 ppm)[80] and the imidazolium proton signal of [IDipp*H*][OTf] (δ = 9.14 ppm). **^{1}H NMR** (CH_2Cl_2/C_6D_6, 500 MHz, 298 K): δ [ppm] = 0.85 (s, 9H, $NH_2C(CH_3)_3$, 1.17 (d, 12H, $^3J_{H,H}$ = 6.8 Hz, $CH(CH_3)_2$), 1.29 (d,12H, $^3J_{H,H}$ = 6.8 Hz, $CH(CH_3)_2$), 1.81 (br, 2H, BH_2), 2.44 (h, 4H, $^3J_{H,H}$ = 6.9 Hz, $CH(CH_3)_2$), 3.45 (s, 2H, $NH_2C(CH_3)_3$, 7.33 (s, 2H, N−C*H*), 7.40 (d, 4H, $^3J_{H,H}$ = 7.8 Hz, Ar*H*), 7.60 (t, 2H, $^3J_{H,H}$ = 7.8 Hz, Ar*H*). **^{11}B NMR** (CH_2Cl_2/C_6D_6, 160.5 MHz, 298 K): δ [ppm] = −21.4 (t, br, BH_2). **^{11}B{^{1}H} NMR** (CH_2Cl_2/C_6D_6, 160.5 MHz, 298 K): δ [ppm] = −21.4 (s, br, BH_2). **^{19}F NMR** (CH_2Cl_2/C_6D_6, 470 MHz, 298 K): δ [ppm] = −78.92 (s, CF_3).

[IDipp•GeH_2BH_2•Py][OTf] (5). IDipp·GeH_2BH_2OTf (**1**) (100 mg, 0.16 mmol, 1 equiv) was suspended in 10 mL of toluene, then the solution of pyridine (13 mg, 0.16 mmol, 1 equiv) was added dropwise. The reaction mixture was stirred for one hour, then all the volatiles were removed *in vacuo* and the product was extracted with DCM. The solution was filtered, the volatiles were removed again *in vacuo* and the product [IDipp·GeH_2BH_2·Py][OTf] (**5**) could be isolated as a white powder (80 mg, 71%). To obtain crystals suitable for the X-ray analysis, a concentrated DCM solution of the product was layered with 3-fold excess of hexane and stored at +9 °C. **^{1}H NMR** (CD_2Cl_2, 400 MHz, 298 K): δ [ppm] = 1.12 (d, 12H, $^3J_{H,H}$ = 6.8 Hz, $CH(CH_3)_2$), 1.20 (d, 12H, $^3J_{H,H}$ = 6.8 Hz, $CH(CH_3)_2$), 2.31 (m, 4H, $^3J_{H,H}$ = 6.8 Hz, $CH(CH_3)_2$), 2.58 (br, 2H, BH_2), 3.44 (t, $^1J_{Ge,H}$ = 4.2 Hz, 2H, GeH_2), 7.33 (d, 4H, $^3J_{H,H}$ = 7.9 Hz, Dipp-Ar*H*), 7.42 (t, 2H, $^3J_{H,H}$ = 7.2 Hz, Py-Ar*H*), 7.54 (s, 2H, N−C*H*), 7.56 (t, 2H, $^3J_{H,H}$ = 7.8 Hz, Dipp-Ar*H*), 7.83 (d, 2H, $^3J_{H,H}$ = 5.3 Hz, Py-Ar*H*), 7.94 (t, 1H, $^3J_{H,H}$ = 7.7 Hz, Py-Ar*H*). **^{11}B NMR** (CD_2Cl_2, 128 MHz, 298 K): δ [ppm] = −14.0 (t, br, BH_2). **^{11}B{^{1}H} NMR** (CD_2Cl_2, 128 MHz, 298 K): δ [ppm] = −14.0 (s, br, BH_2). **^{19}F NMR** (CD_2Cl_2, 376.5 MHz, 298 K): δ [ppm] = −78.80 (s, CF_3). **ESI-MS** (pos. mod., o-DFB): *m*/*z* = 556.29 (100%, [IDipp·GeH_2BH_2·Py]$^+$); **ESI-MS** (neg. mod., o-DFB): *m*/*z* = 148.95 (100%, [CF_3SO_3]$^-$). **Elemental analysis** (%) calculated for $C_{33}H_{45}N_3GeBF_3O_3S$: C: 56.28, H: 6.44, N: 5.97, S: 4.55; found: C: 56.33, H: 6.64, N: 5.93, S: 4.60.

[IDipp•GeH_2BH_2•DMAP][OTf] (6). IDipp·GeH_2BH_2OTf (**1**) (63 mg, 0.1 mmol, 1 equiv) and DMAP (12 mg, 0.1 mmol, 1 equiv) were combined in one flask, then suspended in toluene. The reaction mixture was stirred for one hour, all the volatiles were removed *in vacuo* and the product was extracted with DCM. The solution was filtered, then the volatiles were removed again *in vacuo* and the product [IDipp·GeH_2BH_2•DMAP][OTf] (**6**) could be isolated as a white powder (55 mg, 73%). **^{1}H NMR** (CD_2Cl_2, 400 MHz, 298 K): δ [ppm] = 1.20 (d, 12H, $^3J_{H,H}$ = 7.0 Hz, $CH(CH_3)_2$), 1.30 (d, 12H, $^3J_{H,H}$ = 6.8 Hz, $CH(CH_3)_2$), 2.40 (h, 4H, $^3J_{H,H}$ = 6.9 Hz, $CH(CH_3)_2$), 2.02 (br, 2H, BH_2), 3.04 (s, 6H, DMAP-CH_3), 3.44 (t, $^1J_{Ge,H}$ = 4.4 Hz, 2H, GeH_2), 7.33 (d, 4H, $^3J_{H,H}$ = 7.9 Hz, Dipp-Ar*H*), 7.42 (t, 2H, $^3J_{H,H}$ = 7.2 Hz, DMAP-Ar*H*), 7.54 (s, 2H, N−C*H*), 7.56 (t, 2H, $^3J_{H,H}$ = 7.8 Hz, Dipp-Ar*H*), 7.83 (d, 2H, $^3J_{H,H}$ = 5.3 Hz, DMAP-Ar*H*), 7.94 (t, 1H, $^3J_{H,H}$ = 7.7 Hz, Py-Ar*H*). **^{11}B NMR** (CD_2Cl_2, 128 MHz, 298 K): δ [ppm] = −15.4 (t, br, BH_2). **^{11}B{^{1}H} NMR** (CD_2Cl_2, 128 MHz, 298 K): δ [ppm] = −14.0 (s, br, BH_2). **^{19}F NMR** (CD_2Cl_2, 376.5 MHz, 298 K): δ [ppm] = −78.80 (s, CF_3). **ESI-MS** (pos. mod., o-DFB): *m*/*z* = 599.33 (75%, [IDipp·GeH_2BH_2·DMAP]$^+$); **ESI-MS** (neg. mod., o-DFB): *m*/*z* = 148.95 (100%, [CF_3SO_3]$^-$). **Elemental analysis** (%) calculated for $C_{35}H_{50}N_4GeBF_3O_3S$: C: 56.25, H: 6.74, N: 7.50, S 4.29; found: C: 55.98, H: 6.30, N: 7.59, S: 4.25.

[IDipp•GeH_2BH_2•bipy•BH_2GeH_2•IDipp][OTf]$_2$ (7). IDipp·GeH_2BH_2OTf (**1**) (125 mg, 0.2 mmol, 2 equiv) and bipy (16 mg, 0.1 mmol, 1 equiv) were combined in one flask, then suspended in

https://doi.org/10.1021/acs.inorgchem.6c00556
Inorg. Chem. 2026, 65, 10622−10631

toluene. The reaction mixture was stirred for one hour, then all the volatiles were removed *in vacuo*, the residue was washed with *n*-hexane and then dried. The product [IDipp·GeH_2BH_2•bipy•BH_2GeH_2·IDipp][OTf]$_2$ (**7**) could be isolated as a white powder (116 mg, 83%). To obtain crystals suitable for the SC-XRD a concentrated DCM solution of the product was layered with 3-fold excess of *n*-hexane and stored at +9 °C. **^{1}H NMR** (CD_2Cl_2, 500 MHz, 298 K): δ [ppm] = 1.11 (d, 12H, $^3J_{H,H}$ = 6.8 Hz, $CH(CH_3)_2$), 1.22 (d, 12H, $^3J_{H,H}$ = 6.8 Hz, $CH(CH_3)_2$), 2.30 (h, 4H, $^3J_{H,H}$ = 6.9 Hz, $CH(CH_3)_2$), 2.55 (br, 2H, BH_2), 3.48 (br t, $^1J_{Ge,H}$ = 3.5 Hz, 2H, GeH_2), 7.35 (d, 4H, $^3J_{H,H}$ = 7.8 Hz, Dipp-Ar*H*), 7.47 (s, 2H, N−C*H*), 7.54 (t, 2H, $^3J_{H,H}$ = 7.2 Hz, Py-Ar*H*), 7.59 (t, 2H, $^3J_{H,H}$ = 7.8 Hz, Dipp-Ar*H*), 7.97 (d, 2H, $^3J_{H,H}$ = 6.8 Hz, bipy-Ar*H*), 8.00 (d, 2H, $^3J_{H,H}$ = 6.8 Hz, bipy-Ar*H*). **^{11}B NMR** (CD_2Cl_2, 160.5 MHz, 298 K): δ [ppm] = −12.6 (br, BH_2). **^{11}B{^{1}H} NMR** (CD_2Cl_2, 160.5 MHz, 298 K): δ [ppm] = −12.6 (br, BH_2). **^{19}F NMR** (CD_2Cl_2, 470 MHz, 298 K): δ [ppm] = −78.77 (s, CF_3). **ESI-MS** (pos. mod., o-DFB): m/z = 553.79 (2%, [IDipp·GeH_2BH_2•bipy•BH_2GeH_2·IDipp]$^+$). An intensive signal for IDippH+ (m/z = 389.29) arises due to decomposition in conditions of mass spectrometry; **ESI-MS** (neg. mod., o-DFB): m/z = 148.95 (100%, [CF_3SO_3]$^-$). **Elemental analysis** (%) calculated for $C_{66}H_{88}N_6Ge_2B_2F_6O_6S_2$: C: 56.36, H: 6.31, N: 5.98, S: 4.56; found: C: 56.72, H: 6.87, N: 6.19, S: 4.95.

[IDipp•GeH_2BH_2•dppe•BH_2GeH_2•IDipp][OTf]$_2$ (8). IDipp·GeH_2BH_2OTf (**1**) (125 mg, 0.2 mmol, 2 equiv) and dppe (40 mg, 0.1 mmol, 1 equiv) were combined in one flask, then suspended in toluene. The reaction mixture was stirred for one hour, all the volatiles were removed *in vacuo* and the product was extracted with DCM. The solution was decanted from precipitates, concentrated and stored at −30 °C to obtain the product [IDipp·GeH_2BH_2•dppe•BH_2GeH_2·IDipp][OTf]$_2$ (**8**) as colorless crystals (130 mg, 79%). **^{1}H NMR** (CD_2Cl_2, 500 MHz, 298 K): δ [ppm] = 0.69 (br, 2H, BH_2), 1.22 (d, 24H, $^3J_{H,H}$ = 6.9 Hz, $CH(CH_3)_2$), 1.84 (d, 2H, $^2J_{H,P}$ = 3.0 Hz, $P(CH_2)_2$, 2.34 (h, 4H, $^3J_{H,H}$ = 6.8 Hz, $CH(CH_3)_2$), 3.25 (t, $^1J_{Ge,H}$ = 4.6 Hz, 2H, GeH_2), 7.03 (dd, 4H, $^3J_{H,H}$ = 7.0 Hz, $^3J_{H,P}$ = 11.5 Hz, dppe-*o*-Ar*H*) 7.38 (d, 4H, $^3J_{H,H}$ = 7.8 Hz, Dipp-*m*-Ar*H*), 7.41 (t, 4H, $^3J_{H,H}$ = 7.8 Hz, dppe-*m*-Ar*H*), 7.62 (t, 4H, $^3J_{H,H}$ = 7.8 Hz, Dipp-*p*-Ar*H* + dppe-*p*-Ar*H*), 7.70 (s, 2H, N−C*H*). **^{11}B NMR** (CD_2Cl_2, 160.5 MHz, 298 K): δ [ppm] = −41.8 (br, BH_2). **^{11}B{^{1}H} NMR** (CD_2Cl_2, 160.5 MHz, 298 K): δ [ppm] = −41.8 (br, BH_2). **^{31}P NMR** (CD_2Cl_2, 202.5 MHz, 298 K): δ [ppm] = 18.6 (br, dppe-P). **^{31}P{^{1}H} NMR** (CD_2Cl_2, 202.5 MHz, 298 K): δ [ppm] = 18.6 (br, dppe-P). **^{19}F NMR** (CD_2Cl_2, 470 MHz, 298 K): δ [ppm] = −78.85 (s, CF_3). **ESI-MS** (pos. mod., o-DFB): m/z = 675.32 (9%, [IDipp·GeH_2BH_2•dppe•BH_2GeH_2·IDipp]$^+$). An intensive signal for IDippH+ (m/z = 389.29) arises due to decomposition in conditions of mass spectrometry.; **ESI-MS** (neg. mod., o-DFB): m/z = 148.95 (100%, [CF_3SO_3]$^-$). **Elemental analysis** (%) calculated for $C_{82}H_{104}N_4Ge_2B_2P_2F_6O_6S_2$: C: 59.74, H: 6.36, N: 3.40, S: 3.89; found: C: 58.94, H: 5.89, N: 3.22, S: 3.96.

[$Cp_2Mo_2(CO)_4(\eta^2$-$P_2)$•BH_2GeH_2•IDipp][OTf] (9). IDipp·GeH_2BH_2OTf (**1**) (63 mg, 0.1 mmol, 1 equiv) and [$Cp_2Mo_2(CO)_4(\eta^2$-$P_2)$] (50 mg, 0.1 mmol, 1 equiv) were combined in one flask and suspended in toluene. The reaction mixture was stirred for one and a half hours, all the volatiles were removed *in vacuo* and the product was extracted with DCM. The solution was concentrated, then layered with 3-fold excess of *n*-hexane and stored at +9 °C to obtain the product [$Cp_2Mo_2(CO)_4(\eta^2$-$P_2)$·BH_2GeH_2·IDipp][OTf] (**9**) as red crystals (46 mg, 41%). **^{1}H NMR** (CD_2Cl_2, 500 MHz, 298 K): δ [ppm] = 1.24 (d, 12H, $^3J_{H,H}$ = 6.8 Hz, $CH(CH_3)_2$), 1.35 (d, 12H, $^3J_{H,H}$ = 6.9 Hz, $CH(CH_3)_2$), 1.71 (br, 2H, BH_2), 2.43 (h, 4H, $^3J_{H,H}$ = 6.9 Hz, $CH(CH_3)_2$), 3.56 (m, $^1J_{Ge,H}$ = 4.4 Hz, 2H, GeH_2), 5.28 (s, 10H, Cp-H), 7.43 (d, 4H, $^3J_{H,H}$ = 7.8 Hz, Dipp-Ar*H*), 7.60 (s, 2H, N−C*H*), 7.65 (t, 2H, $^3J_{H,H}$ = 7.8 Hz, Dipp-Ar*H*). **^{11}B NMR** (CD_2Cl_2, 160.5 MHz, 298 K): δ [ppm] = −34.8 (br, BH_2). **^{11}B{^{1}H} NMR** (CD_2Cl_2, 160.5 MHz, 298 K): δ [ppm] = −34.8 (br, BH_2). **^{31}P NMR** (CD_2Cl_2, 202.5 MHz, 298 K): δ [ppm] = −18.5 (d, $^1J_{P,P}$ = 505 Hz, Mo_2P_2), −158.3 (d, $^1J_{P,P}$ = 505 Hz, Mo_2P_2). **^{31}P{^{1}H} NMR** (CD_2Cl_2, 202.5 MHz, 298 K): δ [ppm] = −18.5 (d, $^1J_{P,P}$ = 505 Hz, Mo_2P_2), −158.3 (d, $^1J_{P,P}$ = 505 Hz, Mo_2P_2). **^{19}F NMR** (CD_2Cl_2, 470 MHz, 298 K): δ [ppm] = −78.89 (s, CF_3). **ESI-MS** (pos. mod., o-DFB): m/z = 973.07 (0.3%, [$Cp_2Mo_2(CO)_4(\eta^2$-$P_2)$•BH_2GeH_2·IDipp]$^+$). An intensive signal for IDippH+ (m/z = 389.29) arises due to decomposition in conditions of mass spectrometry.; **ESI-MS** (neg. mod., o-DFB): m/z = 148.95 (100%, [CF_3SO_3]$^-$). **Elemental analysis** (%) calculated for $C_{42}H_{50}N_2GeBF_3O_7SMo_2P_2$: C: 44.99, H: 4.50, N: 2.50, S: 2.86; found: C: 45.75, H: 4.72, N: 2.97, S: 3.22.

Details about anion exchange experiments and the reaction with TMEDA are given in Section 1 of the Supporting Information. The NMR data can be found in Section 2 of the Supporting Information.

X-ray Crystallographic Details

Single-crystal X-ray diffraction experiments were performed on a XtaLAB Synergy R DW system (Rigaku) equipped with a HyPix-Arc 150 detector. Data were collected using Cu−Kα radiation (λ = 1.54178 Å). Data reduction, scaling and absorption corrections were performed using CrysAlisPro[90] (Rigaku). Using Olex2[91] all structures were solved with ShelXT[92] and a least-squares refinement on F^2 was carried out with ShelXL.[93] All non-hydrogen atoms were refined anisotropically. All the hydrogen atoms at the carbon atoms have been located in idealized positions and refined isotropically according to the riding model. Figures were created with Olex2. Crystallographic data and details of the experiments are given in Tables S1, S2 and S3 in the Supporting Information. CIF files with comprehensive information on the details of the diffraction experiments and full tables of bond lengths and angles are deposited in the Cambridge Crystallographic Data Centre under the deposition codes CCDC 2525632−2525639. These data can be obtained free of charge at www.ccdc.cam.ac.uk/conts/retrieving.html (or from the Cambridge Crystallographic Data Centre, 12 Union Road, Cambridge CB2 1EZ, UK; Fax: + 44−1223−336−033; e-mail: deposit@ccdc.cam.ac.uk). Further crystallographic data can be found in Sections 3 and 4 of the Supporting Information.

Computational Details

The geometries of the compounds have been fully optimized with gradient-corrected density functional theory (DFT) in form of Becke's three-parameter hybrid method B3LYP[94,95] with the def2-TZVP[96] all electron basis set. The Gaussian 09[97] program package was used throughout. All structures correspond to minima on their respective potential energy surfaces as verified by computation of second derivatives. Additional information is provided in Section 5 of the Supporting Information.

■ ASSOCIATED CONTENT

Supporting Information

The Supporting Information is available free of charge at https://pubs.acs.org/doi/10.1021/acs.inorgchem.6c00556.

Crystallographic data and computational details (PDF)

Accession Codes

Deposition Numbers 2525632−2525639 contain the supplementary crystallographic data for this paper. These data can be obtained free of charge via the joint Cambridge Crystallographic Data Centre (CCDC) and Fachinformationszentrum Karlsruhe Access Structures service.

■ AUTHOR INFORMATION

Corresponding Author

Manfred Scheer − *Institute of Inorganic Chemistry, University of Regensburg, 93053 Regensburg, Germany;* orcid.org/0000-0003-2182-5020; Email: manfred.scheer@ur.de

Authors

Tatiana N. Parfeniuk − *Institute of Inorganic Chemistry, University of Regensburg, 93053 Regensburg, Germany*

https://doi.org/10.1021/acs.inorgchem.6c00556
Inorg. Chem. 2026, 65, 10622−10631

Matthias T. Ackermann − *Institute of Inorganic Chemistry, University of Regensburg, 93053 Regensburg, Germany*
Christoph Riesinger − *Institute of Inorganic Chemistry, University of Regensburg, 93053 Regensburg, Germany;* Present Address: Imperial College London (White City Campus), London W12 0BZ, United Kingdom

Complete contact information is available at: https://pubs.acs.org/10.1021/acs.inorgchem.6c00556

Author Contributions

T.N.P.: Synthesis and characterization, investigation, X-ray diffraction measurements, structure solution and refinement, computational studies, writing−original draft, review and editing. M.T.A.: Investigation. C.R: Structure solution and refinement, writing−review and editing. M.S.: Conceptualization, writing−review and editing, supervision, resources, project administration, funding acquisition.

Notes

The authors declare no competing financial interest.

■ ACKNOWLEDGMENTS

This work was supported by the German Research Council within the project Sche 384/41-2. Dr. Gábor Balázs and Dr. Robert Szlosek are acknowledged for fruitful discussions. Dr. Lisa Zimmerman is acknowledged for the donation of $[Cp_2Mo_2(CO)_4(\eta^2\text{-}P_2)]$, $[Cp^*_2Mo_2(CO)_4(\eta^2\text{-}As_2)]$ and P_4. This work is dedicated to the memory of Prof. Alexey Y. Timoshkin.

■ REFERENCES

(1) Hoffmann, R. Building Bridges Between Inorganic and Organic Chemistry (Nobel Lecture). *Angew. Chem., Int. Ed.* **1982**, *21* (10), 711−724.
(2) Krüger, C. R.; Rochow, E. G. Polyorganosilazanes. *J. Polym. Sci. A Gen. Pap.* **1964**, *2* (7), 3179−3189.
(3) Allcock, H. R.; Kugel, R. L. Synthesis of High Polymeric Alkoxy- and Aryloxyphosphonitriles. *J. Am. Chem. Soc.* **1965**, *87* (18), 4216−4217.
(4) Krebs, B. Thio- and Seleno-Compounds of Main Group Elements - Novel Inorganic Oligomers and Polymers. *Angew. Chem., Int. Ed.* **1983**, *22* (2), 113−134.
(5) Riedel, R.; Bill, J.; Kienzle, A. Boron-modified Inorganic Polymers-Precursors for the Synthesis of Multicomponent Ceramics. *Appl. Organometal. Chem.* **1996**, *10* (3−4), 241−256.
(6) Jaska, C. A.; Manners, I. Heterogeneous or homogeneous catalysis? Mechanistic studies of the rhodium-catalyzed dehydrocoupling of amine-borane and phosphine-borane adducts. *J. Am. Chem. Soc.* **2004**, *126* (31), 9776−9785.
(7) Trummer, M.; Choffat, F.; Smith, P.; Caseri, W. Polystannanes: synthesis, properties, and outlook. *Macromol. Rapid Commun.* **2012**, *33* (6−7), 448−460.
(8) Cavaye, H.; Clegg, F.; Gould, P. J.; Ladyman, M. K.; Temple, T.; Dossi, E. Primary Alkylphosphine−Borane Polymers: Synthesis, Low Glass Transition Temperature, and a Predictive Capability Thereof. *Macromolecules* **2017**, *50* (23), 9239−9248.
(9) Cornu, D.; Miele, P.; Faure, R.; Bonnetot, B.; Mongeot, H.; Bouix, J. Conversion of $B(NHCH_3)_3$ into boron nitride and polyborazine fibres and tubular BN structures derived therefrom. *J. Mater. Chem.* **1999**, *9* (3), 757−761.
(10) Paine, R. T.; Narula, C. K. Synthetic routes to boron nitride. *Chem. Rev.* **1990**, *90* (1), 73−91.
(11) Malik, M. A.; Afzaal, M.; O'Brien, P. Precursor chemistry for main group elements in semiconducting materials. *Chem. Rev.* **2010**, *110* (7), 4417−4446.
(12) Kher, S. S.; Wells, R. L. A Low Temperature, Solution Phase Synthesis of III-V Semiconductor Nanocrystals. *MRS Proc.* **1994**, *351*, 293−298, DOI: 10.1557/PROC-351-293.
(13) Fujdala, K. L.; Tilley, T. D. An efficient, single-source molecular precursor to silicoaluminophosphates. *J. Am. Chem. Soc.* **2001**, *123* (41), 10133−10134.
(14) Green, M.; O'Brien, P. The synthesis of III−V semiconductor nanoparticles using indium and gallium diorganophosphides as single-molecular precursors. *J. Mater. Chem.* **2004**, *14* (4), 629−636.
(15) Gysling, H. J.; Wernberg, A. A.; Blanton, T. N. Molecular design of single-source precursors for 3−6 semiconductor films: control of phase and stoichiometry in indium selenide (InxSey) films deposited by a spray MOCVD process using single-source reagents. *Chem. Mater.* **1992**, *4* (4), 900−905.
(16) Chandra Sekar, P. V.; Lim, H.; Kim, C. G.; Kim, D. Growth and Characterization of GaN on Sapphire and Porous SWCNT Using Single Molecular Precursor. *Korean. J. Mater. Res.* **2011**, *21* (5), 268−272.
(17) Nöth, H.; Schrägle, W. Beiträge zur Chemie des Bors, XXXII. Zur Synthese dimerer und trimerer Phosphino-borane. *Chem. Ber.* **1965**, *98* (2), 352−362.
(18) Bender, H. R. G.; Niecke, E.; Nieger, M. The first x-ray structure of a phosphasilene: 1,3,4-triphospha-2-sila-1-butene. *J. Am. Chem. Soc.* **1993**, *115* (8), 3314−3315.
(19) Izod, K.; Evans, P.; Waddell, P. G.; Probert, M. R. Remote Substituent Effects on the Structures and Stabilities of P = E π-Stabilized Diphosphatetrylenes $(R_2P)_2E$ (E = Ge, Sn). *Inorg. Chem.* **2016**, *55* (20), 10510−10522.
(20) Nakata, N.; Sekiguchi, A. A stable silaborene: synthesis and characterization. *J. Am. Chem. Soc.* **2006**, *128* (2), 422−423.
(21) Parvin, N.; Ankur; Morgenstern, B.; Scheschkewitz, D. An Authentic Al = Si Double Bond. *Angew. Chem., Int. Ed.* **2025**, *64* (16), No. e202422007, DOI: 10.1002/anie.202422007.
(22) Nakata, N.; Izumi, R.; Lee, V. Y.; Ichinohe, M.; Sekiguchi, A. 1,3-Disila-2-gallata- and -indataallenic Anions $[>Si\text{-}M\text{-}Si<]^-\cdot Li^+$ (M = Ga, In): compounds featuring double bonds between elements of groups 13 and 14. *J. Am. Chem. Soc.* **2004**, *126* (16), 5058−5059.
(23) Petrie, M. A.; Shoner, S. C.; Dias, H. V. R.; Power, P. P. A Compound with a Boron−Arsenic Double Bond. *Angew. Chem., Int. Ed.* **1990**, *29* (9), 1033−1035.
(24) Wang, Y.; Xie, Y.; Wei, P.; King, R. B.; Schaefer, H. F.; Schleyer, P. v. R.; Robinson, G. H. A stable silicon(0) compound with a Si = Si double bond. *Science* **2008**, *321* (5892), 1069−1071.
(25) Sidiropoulos, A.; Jones, C.; Stasch, A.; Klein, S.; Frenking, G. N-heterocyclic carbene stabilized digermanium(0). *Angew. Chem., Int. Ed.* **2009**, *48* (51), 9701−9704.
(26) Jones, C.; Sidiropoulos, A.; Holzmann, N.; Frenking, G.; Stasch, A. An N-heterocyclic carbene adduct of diatomic tin,:Sn = Sn. *Chem. Commun.* **2012**, *48* (79), 9855−9857.
(27) Ghadwal, R. S.; Roesky, H. W.; Merkel, S.; Henn, J.; Stalke, D. Lewis base stabilized dichlorosilylene. *Angew. Chem., Int. Ed.* **2009**, *48* (31), 5683−5686.
(28) Thimer, K. C.; Al-Rafia, S. M. I.; Ferguson, M. J.; McDonald, R.; Rivard, E. Donor/acceptor stabilization of Ge(II) dihydride. *Chem. Commun.* **2009**, No. 46, 7119−7121.
(29) Azhakar, R.; Tavčar, G.; Roesky, H. W.; Hey, J.; Stalke, D. Facile Synthesis of a Rare Chlorosilylene−BH_3 Adduct. *Eur. J. Inorg. Chem.* **2011**, *2011* (4), 475−477.
(30) Rupar, P. A.; Jennings, M. C.; Baines, K. M. Synthesis and Structure of N-Heterocyclic Carbene Complexes of Germanium(II). *Organometallics* **2008**, *27* (19), 5043−5051.
(31) Yao, S.; Xiong, Y.; Driess, M. From NHC−germylenes to stable NHC−germanone complexes. *Chem. Commun.* **2009**, No. 42, 6466−6468.
(32) Rupar, P. A.; Staroverov, V. N.; Baines, K. M. Reactivity Studies of N-Heterocyclic Carbene Complexes of Germanium(II). *Organometallics* **2010**, *29* (21), 4871−4881.
(33) Kocsor, T.-G.; Matioszek, D.; Nemeş, G.; Castel, A.; Escudié, J.; Petrar, P. M.; Saffon, N.; Haiduc, I. Chalcogenobis-

(phosphaalkenyl) germanium and tin compounds. *Inorg. Chem.* **2012**, *51* (14), 7782−7787.
(34) Al-Rafia, S. M. I.; Malcolm, A. C.; McDonald, R.; Ferguson, M. J.; Rivard, E. Trapping the parent inorganic ethylenes H_2SiGeH_2 and H_2SiSnH_2 in the form of stable adducts at ambient temperature. *Angew. Chem., Int. Ed.* **2011**, *50* (36), 8354−8357.
(35) Al-Rafia, S. M. I.; Malcolm, A. C.; McDonald, R.; Ferguson, M. J.; Rivard, E. Efficient generation of stable adducts of Si(II) dihydride using a donor-acceptor approach. *Chem. Commun.* **2012**, *48* (9), 1308−1310.
(36) Ibrahim Al-Rafia, S. M.; Lummis, P. A.; Swarnakar, A. K.; Deutsch, K. C.; Ferguson, M. J.; McDonald, R.; Rivard, E. Preparation and Structures of Group 12 and 14 Element Halide−Carbene Complexes. *Aust. J. Chem.* **2013**, *66* (10), 1235.
(37) Rivard, E.; Merrill, W. A.; Fettinger, J. C.; Wolf, R.; Spikes, G. H.; Power, P. P. Boron-pnictogen multiple bonds: donor-stabilized P = B and As = B bonds and a hindered iminoborane with a B-N triple bond. *Inorg. Chem.* **2007**, *46* (8), 2971−2978.
(38) Swarnakar, A. K.; Hering-Junghans, C.; Nagata, K.; Ferguson, M. J.; McDonald, R.; Tokitoh, N.; Rivard, E. Encapsulating Inorganic Acetylene, HBNH, Using Flanking Coordinative Interactions. *Angew. Chem., Int. Ed.* **2015**, *54* (36), 10666−10669.
(39) Price, A. N.; Nichol, G. S.; Cowley, M. J. Phosphaborenes: Accessible Reagents for the Synthesis of C-C/P-B Isosteres. *Angew. Chem., Int. Ed.* **2017**, *56* (33), 9953−9957.
(40) Helling, C.; Wölper, C.; Schulz, S. Synthesis of a Gallaarsene {HC[C(Me)N-2,6-*i*-Pr_2-C_6H_3]$_2$GaAsCp* Containing a Ga═As Double Bond. *J. Am. Chem. Soc.* **2018**, *140* (15), 5053−5056.
(41) Szych, L. S.; Denker, L.; Feld, J.; Goicoechea, J. M. Trapping an Elusive Phosphanyl-Phosphaalumene. *Chem.-Eur. J.* **2024**, *30* (34), No. e202401326.
(42) Vogel, U.; Timoshkin, A. Y.; Scheer, M. Lewis Acid/Base Stabilized Phosphanylalane and -gallane. *Angew. Chem., Int. Ed.* **2001**, *40* (23), 4409.
(43) Vogel, U.; Hoemensch, P.; Schwan, K.-C.; Timoshkin, A. Y.; Scheer, M. The stabilization of monomeric parent compounds of phosphanyl- and arsanylboranes. *Chem.-Eur. J.* **2003**, *9* (2), 515−519.
(44) Adolf, A.; Zabel, M.; Scheer, M. Main Group Lewis Acid/Base-Stabilised Phosphanylboranes. *Eur. J. Inorg. Chem.* **2007**, *2007* (15), 2136−2143.
(45) Adolf, A.; Vogel, U.; Zabel, M.; Timoshkin, A. Y.; Scheer, M. N-Heterocyclic Carbenes in Lewis Acid/Base Stabilised Phosphanylboranes. *Eur. J. Inorg. Chem.* **2008**, *2008* (22), 3482−3492.
(46) Marquardt, C.; Adolf, A.; Stauber, A.; Bodensteiner, M.; Virovets, A. V.; Timoshkin, A. Y.; Scheer, M. The Lewis Base Stabilized Parent Arsanylborane H_2AsBH_2·NMe_3. *Chem.-Eur. J.* **2013**, *19* (36), 11887−11891.
(47) Marquardt, C.; Hegen, O.; Hautmann, M.; Balázs, G.; Bodensteiner, M.; Virovets, A. V.; Timoshkin, A. Y.; Scheer, M. Isolation and Characterization of Lewis Base Stabilized Monomeric Parent Stibanylboranes. *Angew. Chem., Int. Ed.* **2015**, *54* (44), 13122−13125.
(48) Weinhart, M. A. K.; Lisovenko, A. S.; Timoshkin, A. Y.; Scheer, M. Phosphanylalanes and Phosphanylgallanes Stabilized only by a Lewis Base. *Angew. Chem., Int. Ed.* **2020**, *59* (14), 5541−5545.
(49) Weinhart, M. A. K.; Seidl, M.; Timoshkin, A. Y.; Scheer, M. NHC-stabilized Parent Arsanylalanes and -gallanes. *Angew. Chem., Int. Ed.* **2021**, *60* (7), 3806−3811.
(50) Szlosek, R.; Marquardt, C.; Hegen, O.; Balázs, G.; Riesinger, C.; Timoshkin, A. Y.; Scheer, M. Synthesis of bismuthanyl-substituted monomeric triel hydrides. *Chemical science* **2024**, *15* (36), 14837−14843.
(51) Beer, D. C.; Todd, L. J. The preparation, isomerization, and characterization of some phosphagerma- and arsagermacarboranes. *J. Organomet. Chem.* **1973**, *50* (1), 93−99.
(52) Chen, T.; Duesler, E. N.; Paine, R. T.; Nöth, H. Synthesis of Cage Compounds Containing Boron, Germanium, and Phosphorus Atoms. *Inorg. Chem.* **1997**, *36* (5), 802−808.
(53) Chen, T.; Duesler, E. N.; Paine, R. T.; Nöth, H. Synthesis of Cage Compounds Containing Boron, Tin, and Phosphorus Atoms. *Inorg. Chem.* **1997**, *36* (6), 1070−1075.
(54) Amii, H.; Vranicar, L.; Gornitzka, H.; Bourissou, D.; Bertrand, G. Radical-type reactivity of the 1,3-dibora-2,4-diphosphoniocyclobutane-1,3-diyl. *J. Am. Chem. Soc.* **2004**, *126* (5), 1344−1345.
(55) Nakata, N.; Sekiguchi, A. A stable silaborene: synthesis and characterization. *J. Am. Chem. Soc.* **2006**, *128* (2), 422−423.
(56) Protchenko, A. V.; Birjkumar, K. H.; Dange, D.; Schwarz, A. D.; Vidovic, D.; Jones, C.; Kaltsoyannis, N.; Mountford, P.; Aldridge, S. A stable two-coordinate acyclic silylene. *J. Am. Chem. Soc.* **2012**, *134* (15), 6500−6503.
(57) Protchenko, A. V.; Bates, J. I.; Saleh, L. M. A.; Blake, M. P.; Schwarz, A. D.; Kolychev, E. L.; Thompson, A. L.; Jones, C.; Mountford, P.; Aldridge, S. Enabling and Probing Oxidative Addition and Reductive Elimination at a Group 14 Metal Center: Cleavage and Functionalization of E-H Bonds by a Bis(boryl)stannylene. *J. Am. Chem. Soc.* **2016**, *138* (13), 4555−4564.
(58) Rosas-Sánchez, A.; Alvarado-Beltran, I.; Baceiredo, A.; Hashizume, D.; Saffon-Merceron, N.; Branchadell, V.; Kato, T. The Lightest Element Phosphoranylidene: NHC-Supported Cyclic Borylidene-Phosphorane with Significant B = P Character. *Angew. Chem., Int. Ed.* **2017**, *56* (17), 4814−4818.
(59) Rosas-Sánchez, A.; Alvarado-Beltran, I.; Baceiredo, A.; Saffon-Merceron, N.; Massou, S.; Hashizume, D.; Branchadell, V.; Kato, T. Cyclic (Amino)(Phosphonium Bora-Ylide)Silanone: A Remarkable Room-Temperature-Persistent Silanone. *Angew. Chem., Int. Ed.* **2017**, *56* (50), 15916−15920.
(60) Tholen, P.; Dong, Z.; Schmidtmann, M.; Albers, L.; Müller, T. A Neutral η^5-Aminoborole Complex of Germanium(II). *Angew. Chem., Int. Ed.* **2018**, *57* (40), 13319−13324.
(61) Rao, B.; Kinjo, R. A Cyclic (Alkyl)(boryl)germylene Derived from a Cyclic (Alkyl)(amino)germylene. *Angew. Chem., Int. Ed.* **2019**, *58* (50), 18150−18153.
(62) Rao, B.; Kinjo, R. Crystalline Boragermenes. *Angew. Chem., Int. Ed.* **2020**, *59* (8), 3147−3150.
(63) Omaña, A. A.; Green, R. K.; Kobayashi, R.; He, Y.; Antoniuk, E. R.; Ferguson, M. J.; Zhou, Y.; Veinot, J. G. C.; Iwamoto, T.; Brown, A.; Rivard, E. Frustrated Lewis Pair Chelation as a Vehicle for Low-Temperature Semiconductor Element and Polymer Deposition. *Angew. Chem., Int. Ed.* **2021**, *60* (1), 228−231.
(64) Stuczynski, S. M.; Opila, R. L.; Marsh, P.; Brennan, J. G.; Steigerwald, M. L. Formation of indium phosphide from trimethylindium ($In(CH_3)_3$) and tris(trimethylsilyl)phosphine ($P(Si(CH_3)_3)_3$). *Chem. Mater.* **1991**, *3* (3), 379−381.
(65) Burg, A. B.; Kuljian, E. S. Silyl-Amino Boron Compounds. *J. Am. Chem. Soc.* **1950**, *72* (7), 3103−3107.
(66) Drake, J. E.; Simpson, J. Reactions of monosilylphosphine with boron trichloride, diborane, and monobromodiborane. *Inorg. Chem.* **1967**, *6* (11), 1984−1986.
(67) Lube, M. S.; Wells, R. L.; White, P. S. Preparation and Characterization of Halogen-Boron-Phosphorus Compounds. X-ray Crystal Structures of X_3B·$P(SiMe_3)_3$ and $[X_2BP(SiMe_3)_2]_2$ (X = Cl, Br). *Inorg. Chem.* **1996**, *35* (17), 5007−5014.
(68) Habereder, T.; Nöth, H. Synthesis and Structures of some Trisorganylstannyl Boranes and Triorganylstannyl Borates [1]. *Z. Anorg. Allg. Chem.* **2001**, *627* (4), 789−796.
(69) Kajiwara, T.; Takeda, N.; Sasamori, T.; Tokitoh, N. Insertion of an Overcrowded Silylene into Hydro- and Haloboranes: A Novel Synthesis of Silylborane Derivatives and Their Properties. *Organometallics* **2004**, *23* (20), 4723−4734.
(70) Fan, M.; Paine, R. T.; Duesler, E. N.; Nöth, H. Synthesis and Molecular Structure of Tris[(trimethylsilyl)silyl](diisopropylamino)-(diphenylphosphino)borane. *Z. Anorg. Allg. Chem.* **2006**, *632* (15), 2443−2446.
(71) Habereder, T.; Nöth, H.; Paine, R. T. Synthesis and Reactivity of New Bis(tetramethylpiperidino)(phosphanyl)alumanes. *Eur. J. Inorg. Chem.* **2007**, *2007* (27), 4298−4305.

https://doi.org/10.1021/acs.inorgchem.6c00556
Inorg. Chem. 2026, 65, 10622−10631

(72) Inoue, S.; Leszczyńska, K. An acyclic imino-substituted silylene: synthesis, isolation, and its facile conversion into a zwitterionic silaimine. *Angew. Chem., Int. Ed.* **2012**, *51* (34), 8589−8593.
(73) Wilson, R. J.; Jones, J. R.; Bennett, M. V. Unprecedented gallium-nitrogen anions: synthesis and characterization of $[(Cl_3Ga)_3N]^{3-}$ and $[(Cl_3Ga)_2NSnMe_3]^{2-}$. *Chem. Commun.* **2013**, *49* (44), 5049−5051.
(74) Fernández-Millán, M.; Allen, L. K.; García-Rodríguez, R.; Bond, A. D.; Mosquera, M. E. G.; Wright, D. S. Formation of a unique 'unsupported' hydridic stannate(II). *Chem. Commun.* **2016**, *52* (35), 5993−5996.
(75) Kapitein, M.; Balmer, M.; von Hänisch, C. NHC-stabilized silylphosphino- and silylarsinogallanes. *Phosphorus, Sulfur, and Silicon and the Related Elements* **2016**, *191* (4), 641−644.
(76) Wendel, D.; Porzelt, A.; Herz, F. A. D.; Sarkar, D.; Jandl, C.; Inoue, S.; Rieger, B. From Si(II) to Si(IV) and Back: Reversible Intramolecular Carbon-Carbon Bond Activation by an Acyclic Iminosilylene. *J. Am. Chem. Soc.* **2017**, *139* (24), 8134−8137.
(77) Balmer, M.; Kapitein, M.; von Hänisch, C. Improved reactivity of a cyclic 13/15 compound by increased steric demand. *Dalton Trans.* **2017**, *46* (21), 7074−7081.
(78) Dübek, G.; Franz, D.; Eisenhut, C.; Altmann, P. J.; Inoue, S. Reactivity of an NHC-stabilized pyramidal hydrosilylene with electrophilic boron sources. *Dalton Trans.* **2019**, *48* (17), 5756−5765.
(79) Franz, D.; Szilvási, T.; Pöthig, A.; Inoue, S. Isolation of an N-Heterocyclic Carbene Complex of a Borasilene. *Chem.-Eur. J.* **2019**, *25* (47), 11036−11041.
(80) Ackermann, M. T.; Seidl, M.; Wen, F.; Ferguson, M. J.; Timoshkin, A. Y.; Rivard, E.; Scheer, M. An NHC-Stabilized H_2GeBH_2 Precursor for the Preparation of Cationic Group 13/14/15 Hydride Chains. *Chem.-Eur. J.* **2022**, *28* (3), No. e202103780.
(81) Ackermann, M. T.; Seidl, M.; Grande, R.; Zhou, Y.; Ferguson, M. J.; Timoshkin, A. Y.; Rivard, E.; Scheer, M. A convenient route to mixed cationic group 13/14/15 compounds. *Chem. Sci.* **2023**, *14* (9), 2313−2317.
(82) Ackermann, M. T.; Szlosek, R.; Riesinger, C.; Seidl, M.; Timoshkin, A. Y.; Rivard, E.; Scheer, M. NHC-Stabilized Mixed Group 13/14/15 Element Hydrides. *Chem.-Eur. J.* **2024**, *30* (12), No. e202303680.
(83) Hughes, E. W. The Cystal Structure of Ammonia-Borane, H_3NBH_3. *J. Am. Chem. Soc.* **1956**, *78* (2), 502−503.
(84) Wang, Y.; Quillian, B.; Wei, P.; Wannere, C. S.; Xie, Y.; King, R. B.; Schaefer, H. F.; Schleyer, P. V. R.; Robinson, G. H. A stable, neutral diborene containing a B = B double bond. *J. Am. Chem. Soc.* **2007**, *129* (41), 12412−12413.
(85) Begum, F.; Choudhary, M. A.; Mirza, M. A.; Twamley, B.; Baker, R. J. Synthesis and Structure of the Cyclic Borenium Cation 1,1,3,3-tetramethyl-1,3λ^4,2-diazaborolidin-1-ium chloride. *J. Chem. Crystallogr.* **2018**, *48* (4), 209−212.
(86) Scherer, O. J.; Sitzmann, H.; Wolmershäuser, G. Umsetzung von P_4 mit $(\eta^5\text{-}C_5H_5)(CO)_2Mo{\equiv}Mo(CO)_2(\eta^5\text{-}C_5H_5)$ zu den tetraedrischen molybdänkomplexen $P_n[Mo(CO)_2(\eta^5\text{-}C_5H_5)]_{4-n}$ (n = 2,3). *J. Organomet. Chem.* **1984**, *268* (1), C9−C12.
(87) Scherer, O. J.; Sitzmann, H.; Wolmershäuser, G. $(E_2)_2$-einheiten (E = P, As) als clusterbausteine. *J. Organomet. Chem.* **1986**, *309* (1−2), 77−86.
(88) Moussa, M. E.; Schiller, J.; Peresypkina, E.; Seidl, M.; Balázs, G.; Shelyganov, P.; Scheer, M. The Potential of the Diarsene Complex $[(C_5H_5)_2Mo_2(CO)_4(\mu,\eta^2\text{-}As_2)]$ as a Connector Between Silver Ions. *Chem.-Eur. J.* **2020**, *26* (63), 14315−14319.
(89) Zimmermann, L.; Riesinger, C.; Scheer, M. Potential of Mixed Dipnictogen Molybdenum Complexes in the Self-Assembly of Thallium Coordination Compounds. *Inorg. Chem.* **2024**, *63* (24), 11168−11175.
(90) *CrysAlis PRO*; Oxford Diffraction /Agilent Technologies UK Ltd: Yarnton, England, 2014.
(91) Dolomanov, O. V.; Bourhis, L. J.; Gildea, R. J.; Howard, J. A. K.; Puschmann, H. OLEX2: a complete structure solution, refinement and analysis program. *J. Appl. Crystallogr.* **2009**, *42* (2), 339−341.
(92) Sheldrick, G. M. SHELXT - integrated space-group and crystal-structure determination. *Acta Crystallogr. A* **2015**, *71*, 3−8.
(93) Sheldrick, G. M. Crystal structure refinement with SHELXL. *Acta Crystallogr. C.* **2015**, *71*, 3−8.
(94) Becke, A. D. Density-functional thermochemistry. III. The role of exact exchange. *J. Chem. Phys.* **1993**, *98* (7), 5648−5652.
(95) Lee, C.; Yang, W.; Parr, R. G. Development of the Colle-Salvetti correlation-energy formula into a functional of the electron density. *Phys. Rev. B* **1988**, *37* (2), 785−789.
(96) Weigend, F.; Ahlrichs, R. Balanced basis sets of split valence, triple zeta valence and quadruple zeta valence quality for H to Rn: Design and assessment of accuracy. *Phys. Chem. Chem. Phys.* **2005**, *7* (18), 3297−3305.
(97) Frisch, M. J.; Trucks, G. W.; Schlegel, H. B.; Scuseria, G. E.; Robb, M. A.; Cheeseman, J. R.; Scalmani, G.; Barone, V.; Petersson, G. A.; Nakatsuji, H.; Li, X.; Caricato, M.; Marenich, A.; Bloino, J.; Janesko, B. G.; Gomperts, R.; Mennucci, B.; Hratchian, H. P.; Ortiz, J. V.; Izmaylov, A. F.; Sonnenberg, J. L.; Williams-Young, D.; Ding, F.; Lipparini, F.; Egidi, F.; Goings, J.; Peng, B.; Petrone, A.; Henderson, T.; Ranasinghe, D.; Zakrzewski, V. G.; Gao, J.; Rega, N.; Zheng, G.; Liang, W.; Hada, M.; Ehara, M.; Toyota, K.; Fukuda, R.; Hasegawa, J.; Ishida, M.; Nakajima, T.; Honda, Y.; Kitao, O.; Nakai, H.; Vreven, T.; Throssell, K.; Montgomery, J. A., Jr.; Peralta, J. E.; Ogliaro, F.; Bearpark, M.; Heyd, J. J.; Brothers, E.; Kudin, K. N.; Staroverov, V. N.; Keith, T.; Kobayashi, R.; Normand, J.; Raghavachari, K.; Rendell, A.; Burant, J. C.; Iyengar, S. S.; Tomasi, J.; Cossi, M.; Millam, J. M.; Klene, M.; Adamo, C.; Cammi, R.; Ochterski, J. W.; Martin, R. L.; Morokuma, K.; Farkas, O.; Foresman, J. B.; Fox, D. J. *Gaussian 09*, rev. A.02; Gaussian, Inc.:Wallingford, CT, 2016.

https://doi.org/10.1021/acs.inorgchem.6c00556
Inorg. Chem. 2026, 65, 10622−10631